JOURNAL OF GEOPHYSICAL RESEARCH, VOL. 112, E04S05, doi:10.1029/2006JE002785, 2007



# Meander geometry of Venusian canali: Constraints on flow regime and formation time

V. J. Bray,[1] D. B. J. Bussey,[2] R. C. Ghail,[1] A. P. Jones,[3] and K. T. Pickering[3]

Received 1 July 2006; revised 23 October 2006; accepted 23 January 2007; published 25 April 2007.

[1] The similar meander geometries of Venusian canali and terrestrial rivers imply that the in-channel flow regimes may be comparable. This work details meander geometry measurements from ten lowland canali and compares the extensive data set produced to a variety of solar system channels. The meander properties of Venusian canali do not closely match any channel so far observed on the terrestrial planets. However, analysis of the relationship between meander wavelength and radius of channel curvature confirms previous suggestions that the canali were carved by a low (water-like) viscosity fluid. Whether the canali are due to thermal and/or mechanical erosion of the plains by an exotic lava, or have some other genesis, the dominant meander wavelengths of 11 to 77 km require peak fluid discharge rates of up to $6.6 \times 10^6$ $m^3$ $s^{-1}$, an order of magnitude larger than terrestrial rivers. Slight decrease in width along the channel length was observed in most investigated canali, perhaps reflecting the effect of downstream loss processes. Cyclical variations in the average channel width were observed in some channels; where topographic data are available, these variations apparently correlate with peaks in plains topography. This indicates that the canali remained active, after their initially rapid formation, long enough to interact with the early stages of plains tectonism.

**Citation:** Bray, V. J., D. B. J. Bussey, R. C. Ghail, A. P. Jones, and K. T. Pickering (2007), Meander geometry of Venusian canali: Constraints on flow regime and formation time, *J. Geophys. Res.*, *112*, E04S05, doi:10.1029/2006JE002785.

## 1. Introduction

### 1.1. Canali Characteristics

[2] Canali are simple Venusian channels, distinguishable from sinuous rilles by a longer meander wavelength and radius of curvature [*Baker et al.*, 1992]. The 49 canali-type channels cited to date [*Komatsu et al.*, 1993] tend to be concentrated on smooth lowland plains that have a low density of volcanic and tectonic features (Figure 1) [*Komatsu et al.*, 1993; *William-Jones et al.*, 1998]. Their spatial and temporal relationship to the plains has been used to infer a link between canali formation and plains emplacement [*Komatsu et al.*, 1993; *Komatsu and Baker*, 1994b]. When present, cross-cutting and modification of the canali by tectonism, volcanism and cratering suggests that canali are amongst the oldest features on the plains. Canali are the longest of the Venusian channels, consistently longer than 500 km and reaching up to thousands of kilometers [*Komatsu and Baker*, 1994a]. Combined with their assumed rapid formation, this makes them important stratigraphic markers, allowing widely separated plains units to be temporally linked [*Basilevsky and Head*, 1996].

[1]Department of Earth Science and Engineering, Imperial College London, London, UK.
[2]Applied Physics Laboratory, Laurel, Maryland, USA.
[3]Department of Earth Sciences, University College London, London, UK.


0148-0227/07/2006JE002785$09.00

[3] Bank slopes of ∼6° and depth to width ratios of ∼0.013 [*Kargel et al.*, 1994] make canali similar to low gradient rivers on coarse alluvium [*Schumm*, 1977]. Further similarities to water carved channels include the presence of meander cutoffs and point bars [e.g., *Baker et al.*, 1992; *Komatsu and Baker*, 1996]. Combined with near-constant width along their great lengths [*Baker et al.*, 1997], existing measurements of canali meander geometry show them to be more akin to terrestrial rivers than lava-carved channels [e.g., *Baker et al.*, 1992].

### 1.2. Formation Theories

[4] The morphologic resemblance of canali to terrestrial rivers and submarine channels has led to a wide range of formation theories involving water, turbidity currents and exotic lavas. Taking into account the high surface temperatures and the variety of volcanic features on Venus, the most widely accepted theories on canali origin involve lavas. Formation involving leveed channels of collapsed lava tubes [e.g., *Gregg and Greeley*, 1993] is deemed unlikely due to canali being an order of magnitude wider than any terrestrial counterpart. The presence of point bars implies extensive lateral migration of the canali [*William-Jones et al.*, 1998], indicating equilibrium between erosion and deposition that is not expected with constructional lava tubes or channels [*Carr*, 1974].

[5] *Lang and Hansen* [2006] postulate that canali formed through subsurface fluid flow, involving local stoping and transport of overlying material. The piecemeal nature of the localized erosion is used to explain the observations of

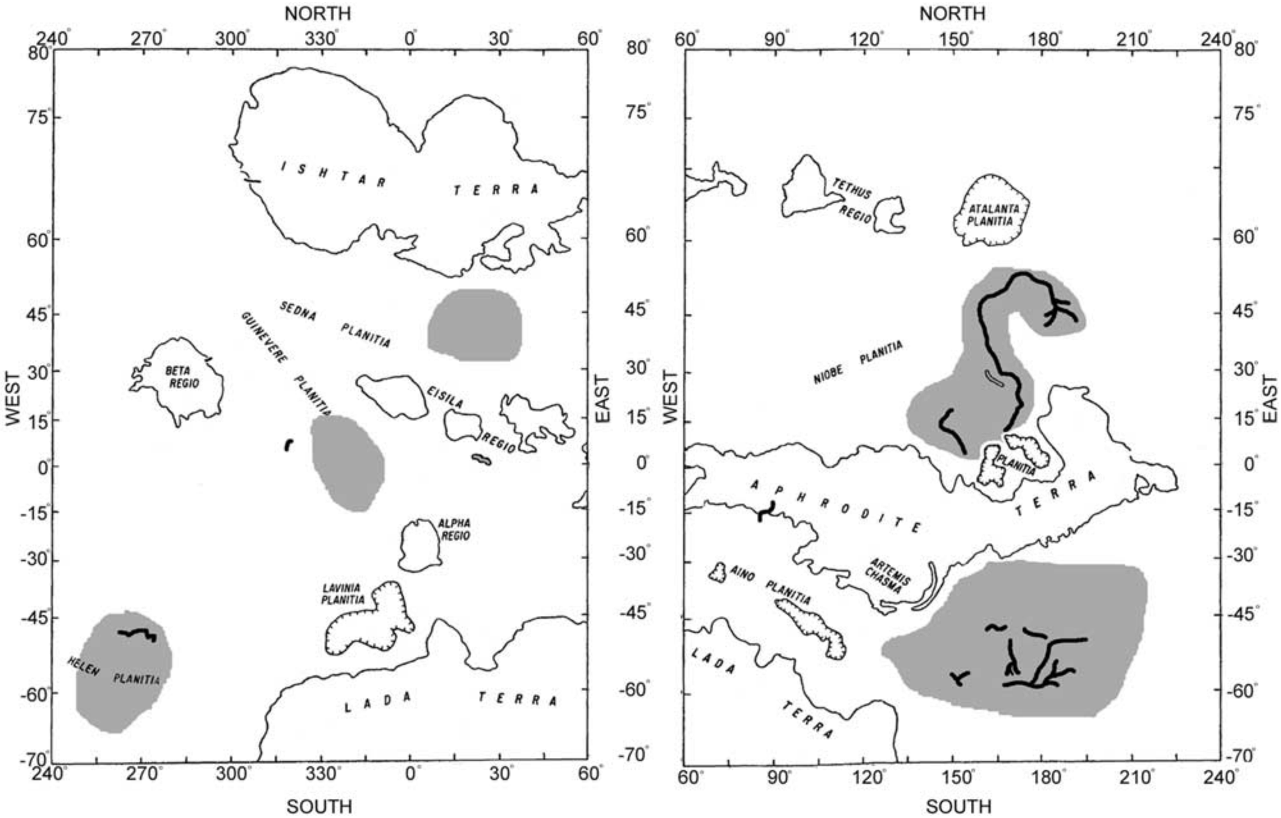


**Figure 1.** Map of Venus in Mercator projection marking the main regions of canali concentration (gray) as identified by *Komatsu et al.* [1993] and *William-Jones et al.* [1998]. The map is modified from *Komatsu et al.* [1993] (with permission from Elsevier) to include the 10 canali-type channels investigated in this work, marked with black lines. Black lines with gray centers mark Nepra Vallis and Huko-ao Vallis.

discontinuous canali segments. However, this process might be expected to produce a more pitted appearance rather than the relatively coherent channels observed.

[6] *Jones and Pickering* [2003] suggested the alternative action of subaqueous sediment gravity flows. However, surface conditions make the presence of standing bodies of liquid water on Venus an impossibility in the current epoch. Although this does not preclude the formation of water-carved channels on Venus during a possibly wetter past, theories involving the water carving of canali are generally considered less plausible than those involving an alternate origin.

[7] The dense Venusian atmosphere may allow for canali formation via atmospheric turbidity currents (D. Waltham, K. T. Pickering, and V. J. Bray, Turbidity currents on Venus, submitted to *Journal of Geophysical Research*, 2007). This process involves erosion via loose particles supported in a self-sustaining gravity current. However, such a mechanism still allows for canali formation in existing conditions, posing the question, where are the younger canali? It is also unclear why the expected strong topographic control is not observed in all cases and along all channel sections.

[8] Although other theories are not disproved, a model involving a combination of thermal and mechanical erosion of the surface rocks by lava is currently the most highly considered formation mechanism [*Baker et al.*, 1992; *William-Jones and Stix*, 1994; *Kargel et al.*, 1994]. Levees and other over-bank deposits demonstrate that canali formation also has a constructional component [*Komatsu et al.*, 1993; *Bussey et al.*, 1995].

### 1.3. Formation Agents

[9] Magmas that have been considered possible candidates for the erosion of canali include tholeiite, olivine nephelenite, komatiite, sulfur, carbonatites and basalts [e.g., *Baker et al.*, 1992; *Komatsu et al.*, 1992; *Gregg and Greeley*, 1993; *Kargel et al.*, 1994; *Lang and Hansen*, 2006]. More in-depth summaries of candidate lavas are given by *Komatsu et al.* [1992] and *Gregg and Greeley* [1993] in which most lavas are rejected as canali forming fluids on the basis of high viscosities. The lowest melting point lavas that have been considered by previous works are alkaline carbonatite and sulfur [*Kargel et al.*, 1994]. The melting point of native sulfur is reduced to 120°C at current Venusian surface pressure [*Robie et al.*, 1978]. Thus, with a viscosity of $7.3 \times 10^3$ Pa s, liquid sulfur provides a possible candidate for canali formation. However, considering the low abundance of sulfur and carbonatite magmas on Earth, it is deemed unlikely that they could be present in sufficient quantities to have formed such extensive channels [*Komatsu

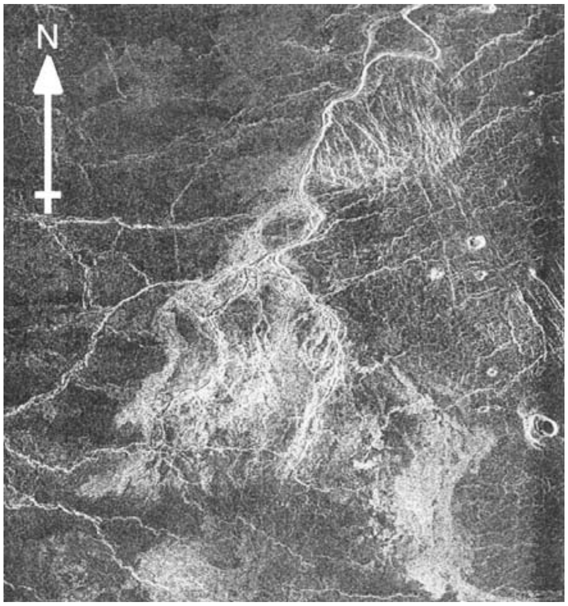


**Figure 2.** Example of a delta-like termination of a canali-type channel. The image is 70 by 94 km and centered about 44°N, 18°E. North is up, and flow direction is assumed to be from NE to SW.

*et al.*, 1992]. Currently, no known lava is universally accepted as having formed the channels. Instead, a low viscosity, low melting temperature exotic lava, extruded under exotic eruption conditions is required [*Komatsu et al.*, 1992, 1993].

### 1.4. Quantitative Analysis of Canali

[10] In order to assess the suitability of the different formation theories, it is necessary to analyze canali morphology. The meander geometry of a channel provides information on the rheological properties of the fluid carving the channel, and the flow regime within it. However, due to the relatively low number of measurements collected in previous works [e.g., *Baker et al.*, 1992; *Komatsu and Baker*, 1994a], canali analysis has remained largely qualitative, making theories of their formation difficult to assess objectively.

[11] This work includes measurements of the radius of curvature, width, meander wavelength and sinuosity at different distances from the ''source'' of 10 lowland canali-type channels (mapped in Figure 1). The data set includes over 5700 data points, allowing for much more robust comparisons between the meander geometry of Venusian canali and of other channels on the terrestrial planets.

[12] As contrasting ideas of canali formation exist, we present findings without support of one specific theory. It is instead our intention that the data may be used by future works to better understand the canali formation process and the properties of canali forming fluids. Analysis of meander geometry in this work therefore uses techniques that have been applied to both volcanic and aqueous solar system channels. The use of different techniques is to demonstrate the flexibility of the data set, while providing further example of how application of river/lava flow dynamics can be used to study canali-type channels.

## 2. Methodology

### 2.1. Channel Selection and Flow Direction

[13] To allow the general trend of canali-type channels to be assessed, a number of channels were investigated. Figure 1 shows the location of the 10 lowland canali included in this work. For ease of measurement and reduction of errors, poorly defined and relatively thin canali (<250 m) were not included in this study.

[14] Before measurements were taken, a flow direction was assigned to each canali; this was done on the basis of several factors. Delta-like deposits and other obvious depositional features (Figure 2) were assumed to mark channel termini; the flow direction would then be recorded as flowing toward this point. Without a defined source or terminus, the determination of the flow direction relies upon the analysis of in-channel flow features, which is beyond the scope of this work. Instead, a probable flow direction was based on the arrangement of ''minor'' channels, such as A, B and C in Figure 6.

[15] Assuming such subsidiary channels are distributaries instead of tributaries, we have inferred an X to X' flow direction in Figure 5 on the premise that they will be branching out in a downstream direction. It should be noted that such an assumption is questionable, and therefore the flow direction noted in this work is a suggested direction only. Further investigation into the local topography could shed light on whether the branches shown in Figures 5 and 6 are indeed distributaries. It is expected that, if the mean topographic elevation local to each branch increases with distance from the main channel, then the subsidiary channels are most likely tributaries, bringing more fluid to the main channel from uphill areas. Conversely, a decrease in topography would confirm the role of the new branches as distributaries, spreading the canali forming fluid to other lowland areas.

### 2.2. Measurements

[16] This work includes measurement of width, radius of curvature, meander wavelength and sinuosity with distance from the ''source'' of each investigated canali, as summarized in Figure 3. Errors in our measurements were calculated on the basis of their reproducibility and the resolution of the Magellan radar data (75 m per pixel). In areas where channel sections are obscured by impact, lava flows or data gaps, the channel was measured as straight (sinuosity = 1). The total channel lengths recorded in this work should therefore be considered as a lower bound.

[17] Measurements were taken at every point of maximum and minimum curvature (a and b in Figure 3, respectively) of the canali from ''source'' to ''terminus.'' In cases where channel levees were discernable on both sides, the width of the canali was taken to be from levee peak to levee peak (see *Bussey et al.* [1995] for an explanation of the radar signature of levees). Otherwise, the edge of the canali was taken to be the visible discontinuity between the plains and the channel. When one or both sides of the canali were not reliably discernable, width

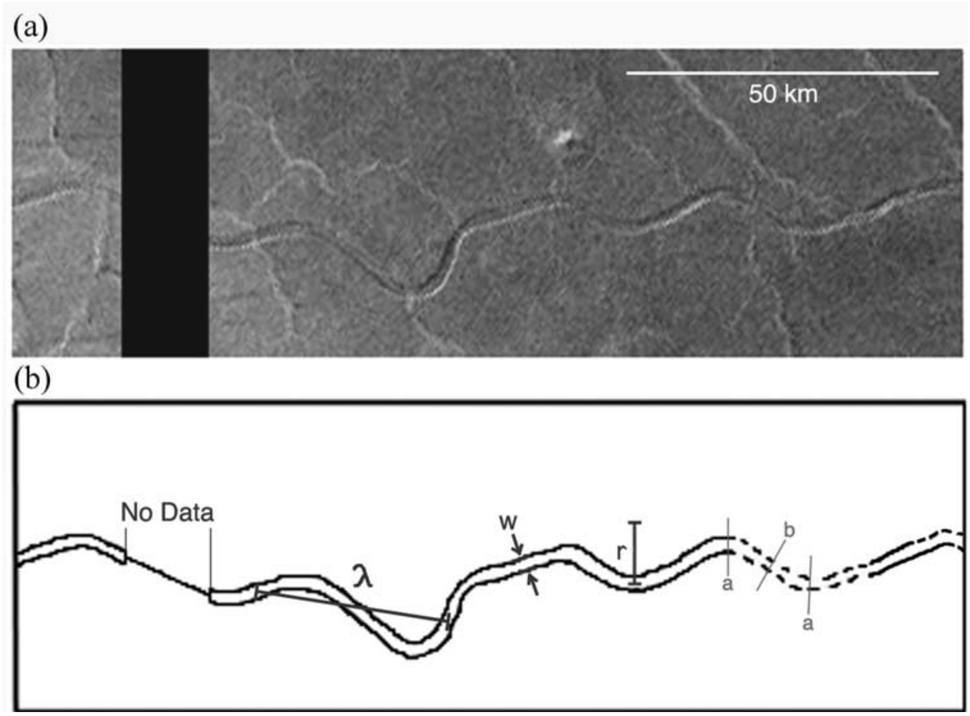


**Figure 3.** (a) Section of a typical canali-type channel, Baltis Vallis. The image is centered at ~50°N, 167°E. (b) A trace of the channel section detailing what was measured and how areas of questionable channel width (dashed line) and no data were recorded during data collection. Width measurements, w, were taken at every point of maximum, a, and minimum curvature, b. Radius of curvature, r, was measured at all points of maximum curvature. Meander wavelength, λ, was measured between alternate points of minimum curvature. The actual channel length, l, between these two points was also recorded and used to calculate sinuosity, s, via s = l/λ. Distance from the "source" of each channel was recorded at each point of minimum and maximum curvature so that variation of λ, w, r, and s with downstream distance could be assessed.

measurements were not taken in order to prevent spurious results.

### 2.3. Nepra Vallis and Huko-ao Vallis

[18] In order to assess the similarity of canali to other Venusian channels using directly comparable data sets, our work includes measurements of two other channels. *Baker et al.* [1992] state that a canali-type channel ought to have "a high width to depth ratio and remarkably constant width." Huko-ao Vallis and Nepra Vallis (Figure 4) both display characteristics more akin to other Venusian lava channels than canali, showing a noticeable increase in width along their relatively short lengths (Figure 9). Summarized measurements of these channels are included alongside the main data set in Table 1; however, Nepra and Huko-ao Vallis are then considered separately from the canali-type channels in the next section.

## 3. Results

### 3.1. Flow Rate and Volume

[19] Previously recorded as 6800 km [*Baker et al.*, 1992], Baltis Vallis is the largest of the Venusian canali and the longest channel recorded on the terrestrial planets [*Komatsu and Baker*, 1996]. As a result, it has been used as a test case for canali formation theories, as the proposed mechanism must be capable of forming a channel in excess of 6800 km [e.g., *Komatsu et al.*, 1992]. This large distance implies the flow of a massive volume of fluid (~$10^{12}$ $m^3$) [*Komatsu et al.*, 1992], a factor which further restricts formation theories, as there must be a suitably large source of material available that is capable of flowing such a distance.

[20] Figure 5 displays the main trunk of Baltis Vallis. Inclusion of branches in the boxed area raise the total measurable length of the canali-type channel to 7181 ± 14 km. A faint channel outline extending to X' is also marked. If a continuation of the channel, this would increase Baltis Vallis's total length to 7312 ± 14 km. The channel is likely to have originally reached farther than this, as the branch is overprinted by volcanic units. The extra length proposed by our work calls for a larger volume of fluid involved in canali-formation. It also requires a canali forming process capable of carving channels longer by a further 300 km than previously realized.

[21] Canali are assumed to have formed rapidly due to their shallow depths and long wavelengths (V. R. Baker, personal communication, 2006). A high discharge rate is necessary when considering their use as stratigraphic markers [*Basilevsky and Head*, 1996] as this requires both source and terminus ends of the channel to have comparable age. However, the presence of braiding and other small-scale channel features indicate that the flow rate was not always high, instead requiring a velocity of ~1 m $s^{-1}$ for

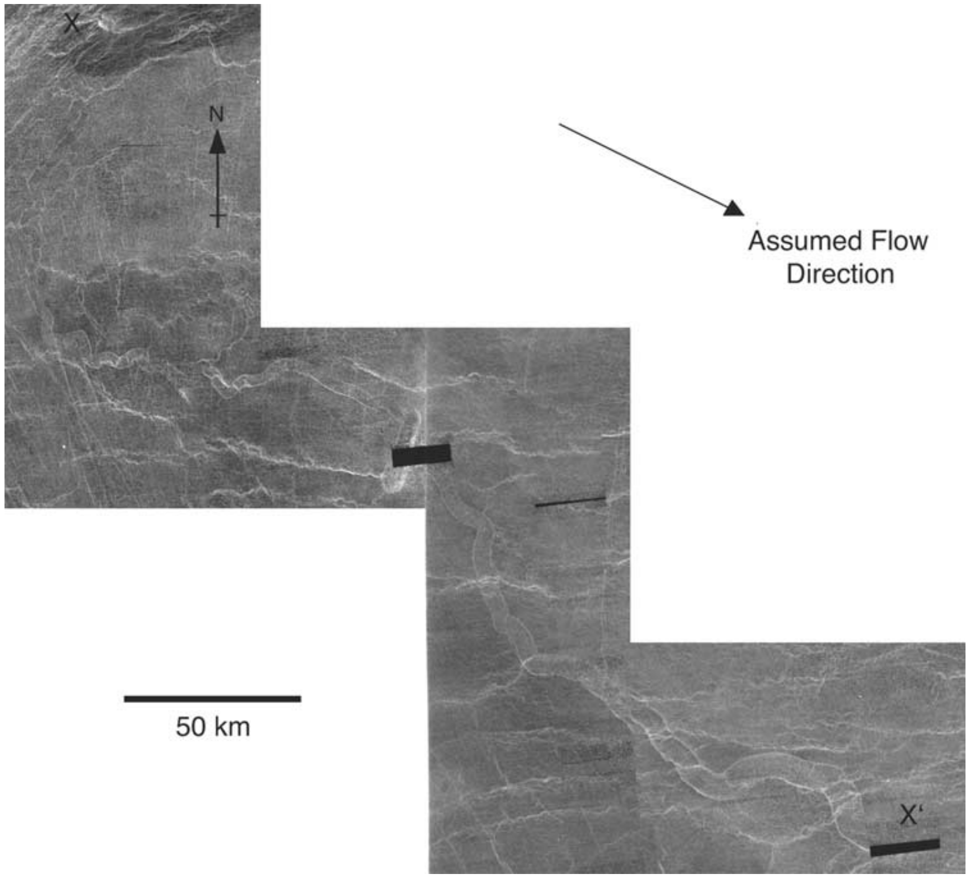


**Figure 4.** Image of Nepra Vallis. Flow direction was taken as X to X'. The width increase along this length (427.5 km) is significant compared to what would be expected of a canali-type channel. The image is centered at ~1.4°N, 24.2°E. North is up.

the formation of these features [*William-Jones et al.*, 1998]. Cross-sectional profiles of Baltis Vallis created by *Oshigami and Namiki* [2005] show the presence of an inner channel, indicative of at least two stages of channel formation, as reported for Martian outflow channels [*Williams and Malin*, 2004].

[22] The presence of levees and over-bank flood deposits imply that the flow within canali-type channels reached bank-full at some stage during their formation. Assuming that the flow regime of canali was dominated by bank erosion and sediment transport processes, terrestrial river dynamics may offer a means to estimate this bank-full

**Table 1.** Summary of Meander Geometry Measurements[a]

| | Lat. | Long. | Measured Length, km | Width, km | Meander Wavelength, km | Radius of Curvature, km | Sinuosity Range | Data Points |
|---|---|---|---|---|---|---|---|---|
| Canali | | | | | | | | |
| Baltis Vallis | 37.3 | 161.4 | 7181 | 0.9–3.4 | 11–243 | 4 – 375 | 1.01–2.69 | 1260 |
| Ikhwezi Vallis | 16 | 147.8 | 1916 | 0.3–3 | 7.0–99 | 1.0–31 | 1.03–3.75 | 1096 |
| Tingoi Vallis | 6 | 318.6 | 675 | 0.45–2.1 | 15–89 | 1.5–72 | 1.01–2.27 | 172 |
| Lusaber Vallis | −47.5 | 164 | 938 | 0.25–1.4 | 7.0–46 | 3.0–71 | 1.02–2 | 648 |
| Sinann Vallis | −49 | 270 | 1095 | 0.5–2.3 | 8.0–59 | 1.5–24 | 1.03–2 | 488 |
| Austrina Vallis | −49.5 | 177 | 529 | 0.68–3.8 | 31.0–90 | 7.5–71 | 1.02–1.21 | 172 |
| Citlalpul Vallis | −51.8 | 187 | 2257 | 0.3–1.8 | 14–90 | 1.5 –64 | 1.01–1.5 | 729 |
| Nahid Valles | −55.1 | 171 | 949 | 0.9–2.6 | 22–372 | 6.0–368 | 1.03–1.3 | 229 |
| Xulab Vallis | −57.5 | 186 | 1610 | 0.3–1.6 | 15–112 | 4.0–83 | 1.01–1.25 | 476 |
| Kumsong Vallis | −59 | 152.5 | 525 | 0.25–1.9 | 14.0–68 | 3.0–53 | 1.1–1.94 | 160 |
| Other channels | | | | | | | | |
| Huko-ao Vallis | 28 | 166.5 | 364 | 1.95–6.6 | 33–64 | 16.5–64 | 1.06–1.4 | 80 |
| Nepra Vallis | 1.4 | 24.2 | 428 | 2.7–9.2 | 9.0–65 | 3.0–60 | 1.1–1.25 | 204 |

[a]Channel names were taken from the USGS database of Venus nomenclature. Measured lengths are recorded as the maximum length for which channel geometry measurements could be confidently made. As a result, some channels will extend for greater lengths than recorded here.

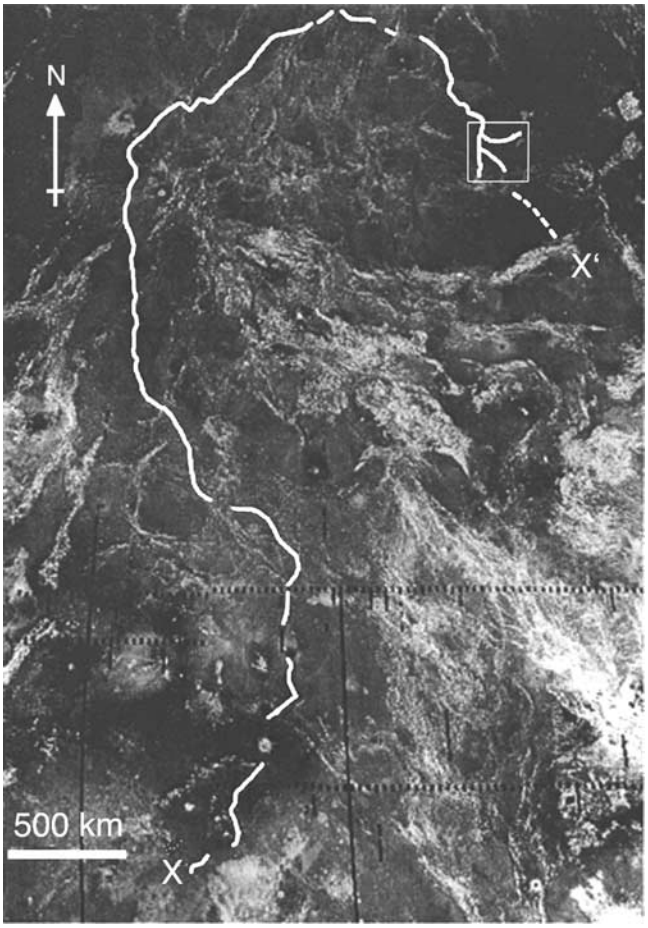


**Figure 5.** Outline of Baltis Vallis, modified from *Komatsu and Baker* [1994b] (with permission from Elsevier). The image covers latitude 9–53°N and longitude 150–200°E. Assumed flow direction is X to X'. Inclusion of the branches in the boxed area (close-up included as Figure 6) allows the channel to be traced an additional 300 km farther than previously mapped. A faint channel outline (dashed line extending to X') is also marked as a suggested continuation to the channel; this would increase Baltis Vallis's total length to 7312 ± 14 km.

(peak) discharge rate on the basis of meander wavelength. An empirical relationship between the dominant meander wavelength of river channels, $\lambda$, and their bank full discharge rate, Q, has been noted by *Dury* [1964]. The two variables are related by equation (1):

$$\lambda = 30Q^{1/2} \qquad (1)$$

The dominant meander wavelength for the canali investigated in this work ranges from 11 ± 2.4 to 77 ± 2.4 km for different channels, relating to a peak discharge rate of $1.4 \times 10^5$ to $6.6 \times 10^6$ $m^3$ $s^{-1}$, as plotted in Figure 7.

[23] The estimates obtained in this work confirm the data of *Kargel et al.* [1994], in which the general estimated discharge of canali is an order of magnitude larger than the terrestrial river discharge recorded by *Leopold and Wolman* [1957]. If accurate, these values suggest that canali formation was a large-scale, initially rapid process involving vast quantities of lava (or other formation agent). The implied high effusion rate requires these volumes to be readily available. The need for such large volumes of canali-forming agent presents further problems for volcanic formation theories; especially those involving carbonatites and sulfur as these lavas are not available in sufficient quantities on Earth [*Komatsu et al.*, 1992].

[24] Consideration of both large and small-scale features suggests that an initially high discharge rate was followed by a prolonged slower flow. Draining of the fluid from the channel was likely a gradual process, allowing for the formation of the inner channels.

### 3.2. Meander Geometry and Flow Viscosity

[25] The characteristics of a channel, such as meander wavelength and braiding habit, relate to the physical behavior of the channel forming fluid [*Baker et al.*, 1992]. This is not a simple relationship as the flow properties can be affected by surface slope, local gravity, discharge rate and flow duration, among others. However, *Baker et al.* [1992] found a strong dependence of lava channel morphology upon fluid viscosity; this simplified relationship has subsequently been used to infer that the canali-carving fluid was of water-like viscosity [*Kargel et al.*, 1994]. The results presented in Figure 8 are consistent with this conclusion. Accurate interpretation of Figure 8 is complicated due to the other factors affecting the behavior of the channel forming fluid. However, the separation of the volcanic and aqueous channels into two distinct groups in Figure 8b allows a simple comparison to be made: the slope of the trend lines reflects the different viscosities of the channel forming fluids such that higher viscosity fluids generally have a steeper trend line.

[26] Although a strict relation to the radius of curvature was not evident due to the wide range of meander wavelengths recorded in this work, a general trend is followed by each channel, and the data set as a whole, allowing a trend line to be tentatively inferred. The variation of canali wavelength with radius of curvature does not match any other solar system channel trend, as illustrated in Figure 8b. However, the trend line gradient is most similar to that of terrestrial rivers, indicating that the canali carving fluid was of a similar viscosity to water. The trend lines Nepra and Huko-ao Vallis fall between the volcanic and aqueous domains in Figure 8b, but with a gradient closer to that of Venusian and lunar rilles than the main data set. This suggests that the fluid carving these channels is also less viscous than any silicate lava, and only slightly more viscous than water.

[27] It is expected that the trend lines marking the relationship between meander wavelength and radius of curvature for all channels carved by a Newtonian fluid will trend to zero as a result of the fluid rheology. The radius of curvature ($y$ axis) $\sim$5 intercept of the canali data set in Figure 8b is therefore unexpected. Although two possible explanations for this result are outlined here, it is accepted that it is difficult to explain reliably without further investigation and may be anomalous. If due to errors during data collection, the same effect should be expected for Nepra Vallis and Huko-ao Vallis, which is not the case. Nahid Vallis has a trend line that does progress back to the graph

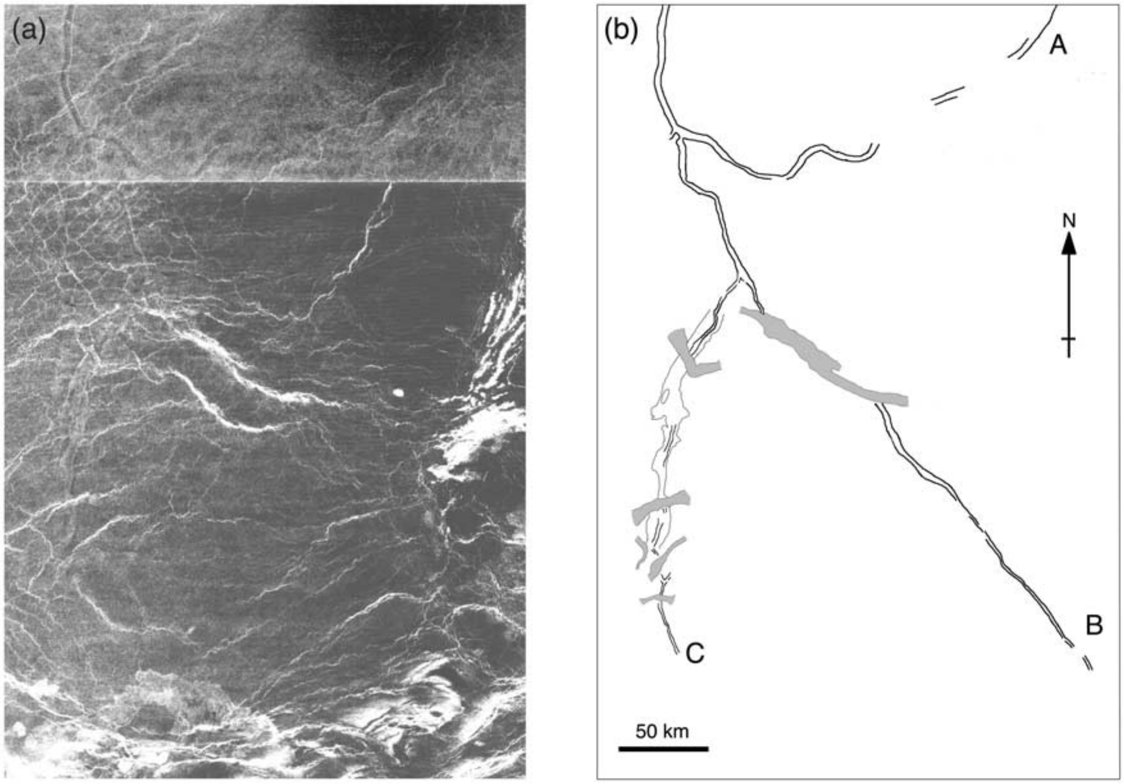


**Figure 6.** (a) Close-up of the boxed area in Figure 5 showing a section of Baltis Vallis. The image is centered ~47°N, 184°E. North is up. The faint continuation of branch B recorded in Figure 5 is not included as it cannot be resolved with this image size. (b) Simplified tracing of the main trunks of Baltis Vallis; small-scale braiding and branching are not included, although it should be noted that this area is heavily marked by other possible channel branches and braiding sections. The path of the canali-type channel is difficult to pick out in Figure 6a. As a result, although areas of indeterminate width were recorded with dashed lines during data collection, solid black lines were used in this figure so that the path of this poorly defined channel section could be marked. Thinner black lines around branch C mark over-bank deposits. Gray areas denote where fractures or other features have obscured the channel.

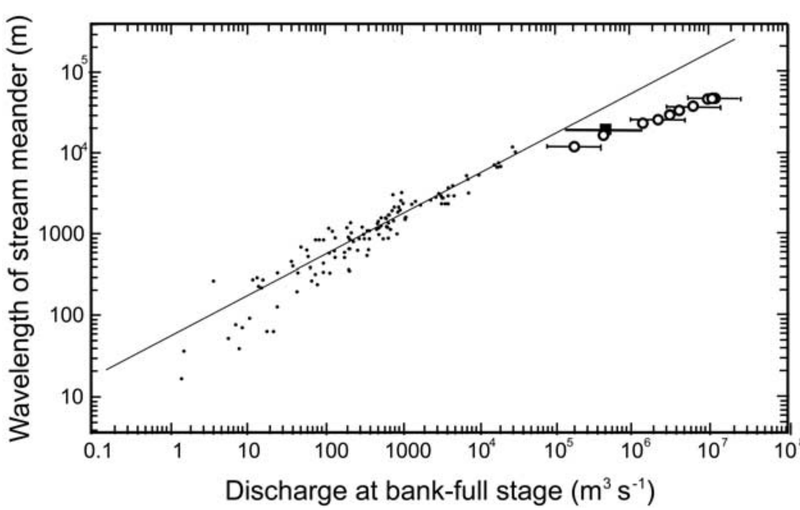


**Figure 7.** Plot of channel discharge and dominant meander wavelength, modified from *Kargel et al.* [1994] (with permission from Elsevier). Black circles mark terrestrial river data from *Leopold and Wolman* [1957] and *Dury* [1964]. The trend line applies to the terrestrial river data. Calculations of discharge from this work using equation (1) are marked with white circles, and a representative number of error bars are included. The datum from *Kargel et al.* [1994] is included as a black square, also with error bar.

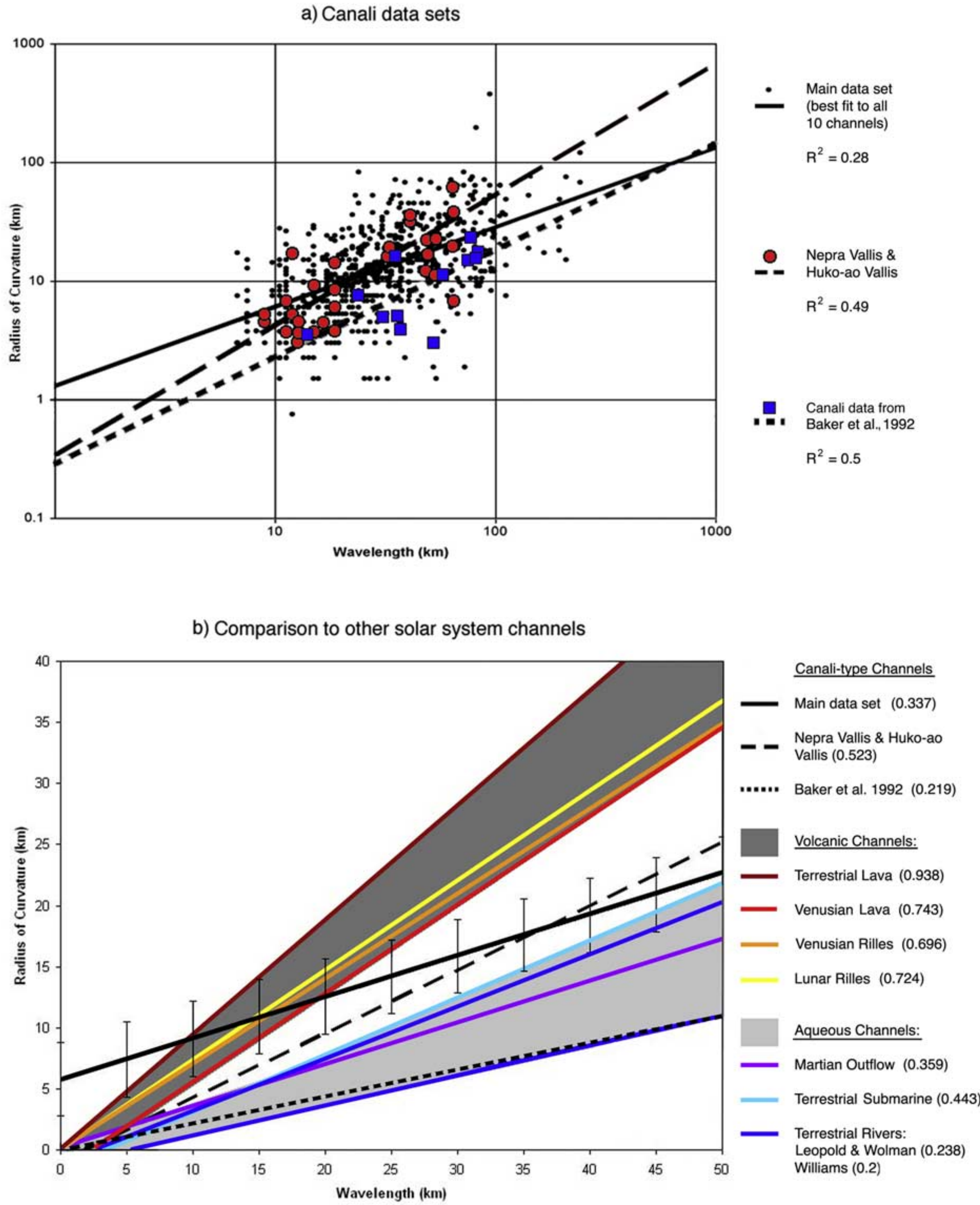


**Figure 8.** Graphs showing the relationship between wavelength and radius of curvature for the combined canali data set. (a) Black spots denote the 10 canali-type channels; red circles mark data points from Nepra Vallis and Huko-ao Vallis. Data points from *Baker et al.* [1992] have been included for comparison as blue squares. Trend lines for each have been included. (b) Comparison of canali data with aqueous and volcanic channels. Data points have been removed for clarity. Data for terrestrial lava, Venusian and lunar rilles, and Venusian lava channels were taken from *Komatsu and Baker* [1994b], terrestrial submarine channel data are from *Clark and Pickering* [1996], Martian outflow channel data are from *Kereszturi* [2003], and terrestrial river data are from *Leopold and Wolman* [1960] and *Williams* [1986]. The trend lines have been included for comparison, and the trend line gradients have been included in parentheses in the key.

origin as expected. However, the other 9 canali-type channels investigated all follow the main trend, showing a minimum radius of curvature between 4 and 30 km.

[28] Given that this result is therefore an accurate reflection of the meander geometry of canali-type channels, the relatively large radius of curvature at the smallest meander wavelengths could be an artifact of the extensive fracturing on the Venusian plains. The prominent fractures, if active at or before canali formation, could have dictated small sections of the flow to some extent. This would result in later generations of meanders (which have smaller radii of curvature and shorter wavelengths) being more obviously affected than longer wavelength meanders, thus off-setting the trend line. The comparatively short length and large width of Nepra Vallis and Huko-ao Vallis may not have been as effected by this proposed process, and hence have meander wavelength vs. radius of curvature trend lines that trend to zero. Any such fracture-related explanation for the high *y* axis intercept of the canali-type channel trend line in Figure 8b will only be confirmed with further investigation into the relative ages of canali formation and tectonic activity on the plains.

[29] Alternatively this trend could reflect a variance in the erosional power of the canali-carving fluid as distance from the "source" increases. The y-intercept of the canali trend line in Figure 8b shows that the largest ratio of radius of curvature to meander wavelength occurs at the smallest wavelengths. As a general increase in meander wavelength with distance from the source of canali-type channels has been noted [*Bussey et al.*, 1995; this work], it follows that the largest ratio of radius of curvature to wavelength also occurs closest to the channel "source." This may suggest changes in flow properties, or that different erosional mechanisms are more prevalent at the source compared to farther downstream (e.g., mechanical erosion of the canali by a lava could be enhanced close to the vent by higher rates of thermal erosion).

### 3.3. Channel Width and Viscosity Variation

[30] Changes in the width of a lava channel reflect changes in the rheological properties of the lava as distance from the vent increases [*Rossi*, 1997]. In their lava morphology model, based on both terrestrial and Martian lavas, *Garry and Gregg* [2005] demonstrated that, independent of scale, lava flows tend to broaden downstream (note that this model was developed for steeper topographic gradients than Venusian canali terrains). River channels broaden and deepen downstream due to tributaries adding to the volume of fluid as distance from the source increases. However, in areas of increasing substrate resistance, river channels have been recorded to narrow downstream [e.g., *Wohl and Achyuthan*, 2002]. The morphology of different solar system channels is presented in more detail by *Komatsu and Baker* [1996].

[31] Canali are known for their near-constant widths along their lengths [*Komatsu and Baker*, 1992, 1994a], which implies that the canali-carving fluid retained a near-constant viscosity and flow volume during the channel forming process. If volcanic, this near-constant viscosity adds significant restrictions to the nature of the canali-carving fluid since it must be able to flow over 7000 km without experiencing significant cooling, which would otherwise lead to crystallization. The presence of crystals in any magma, whether silicate or carbonatite melt, will cause an increase, albeit modest, in viscosity, making it less able to behave like water [e.g., *Genge et al.*, 1995]. Therefore any lava proposed as the canali-forming fluid must have a liquidus at or below the ambient temperature, and a solidus as low as possible, in order to not experience significant crystallization. This is possible if the Venusian climate was hotter in the past [*Bullock and Grinspoon*, 2001], or if the canali were formed by a low viscosity lava of low (< 700 K) melting point, as suggested by *Kargel et al.* [1994]. Another possibility is that the temperature of the lava/fluid may be maintained above its solidus, and crystallization inhibited, by possible exothermic reactions between the fluid and the substrate; this hypothesis is yet to be investigated.

[32] The two non-canali-type channels included in this work, Nepra and Huko-ao Vallis, show increases of 5.0 and 4.3 km in average width over channel lengths of 430 and 360 km, respectively. The width increase of these two channels is interpreted to be the result of viscosity increase of the channel-forming lava as it cools. The width variance of the canali-type channels is less dramatic, with Tingoi Vallis showing only a 13 m decrease in average channel width along its 680 km length. The canali widths do not all remain as constant as this example and down stream width changes of as much as 500 m over a 530 km long channel are observed (Kümsong Vallis). This variable trend in canali width with distance is shown in Figure 9.

[33] Providing that the interpretation of subsidiary channels as distributaries is correct, 9 of the 10 investigated canali-type channels show near constant or decreasing channel width along their lengths. The variance in the magnitude of this trend suggests that the controlling factor is not solely inherent to the channel formation process or to the properties of the canali-carving fluid. Instead, distributaries, tributaries and over-bank flow could affect the flow volume of the main channel. If this is indeed the case, the narrowing of the canali could reflect the effect of downstream loss processes, with the magnitude of the downstream narrowing reflecting the magnitude of the losses (V. R. Baker, personal communication, 2006). A noticeable loss process observed during this investigation involved over-bank flow from locally breached canali margins (noted in Figure 6b). The material diverted from the main channel after levee-breach decreases the volume of fluid continuing into downstream regions, leading to narrowing of the main channel. Additional to any changes in the flow volume, the changes in channel width could reflect variances in the gradient of the slope over which the canali originally formed, as steeper gradients will generally produce thinner channels [*Hulme*, 1974]. Changes in the physical properties of the flow and the substrate will also affect channel width, as noted earlier.

### 3.4. Small-Scale Variation of Channel Width

[34] Along the length of each canali, several peaks in width are obvious (e.g., the first data point recording a 3.75 km width for Austrina Vallis, Figure 9). It is possible that these outliers are the result of pooling in topographic lows. However, this would likely form a circular shape to that section of the channel, which is not observed. Instead,

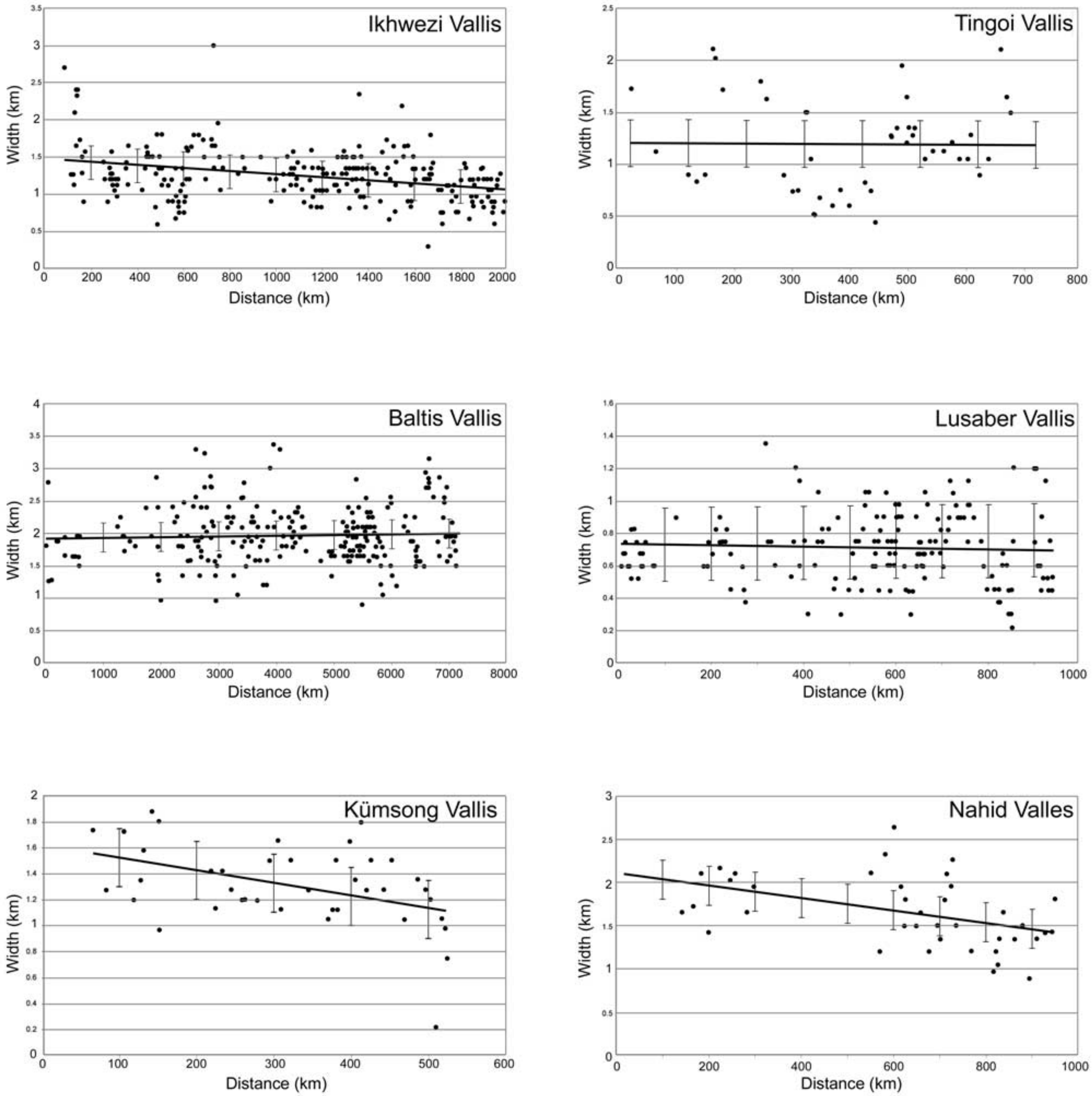


**Figure 9.** Width variation with distance for the individual channels investigated in this work. Linear trend lines are used to show the general magnitude of narrowing or broadening downstream. Large-scale cyclic variance in the average channel width is particularly prominent in Xulab Vallis, Tingoi Vallis, Citlalpul Vallis, and the far downstream half of Lusaber Vallis.

widening of the channel could have occurred at points of tectonic extension. To further investigate this, a better match between topography data and our width measurements is needed, and is not entered into in this paper.

[35] Figure 10b illustrates a crude cyclical variation in average width along the length of the channel, which has been identified in some of the other canali and is particularly prominent in this example. Close examination of the areas of average width maxima and minima show that this result is not an artifact of subsequent modification of the channel by fracturing or infill, but rather a characteristic developed during canali formation itself. A similar width variation has been noted in terrestrial river channels and attributed to varying rates of erosion [*Schumm and Hadley*, 1957].

[36] This width variation could perhaps be explained if canali were of constructional volcanic origin since lava tubes can prolong their total flow through a series of flow front ‘‘breakouts’’: For most of the tube length the flow remains insulated and of constant width. However, if the

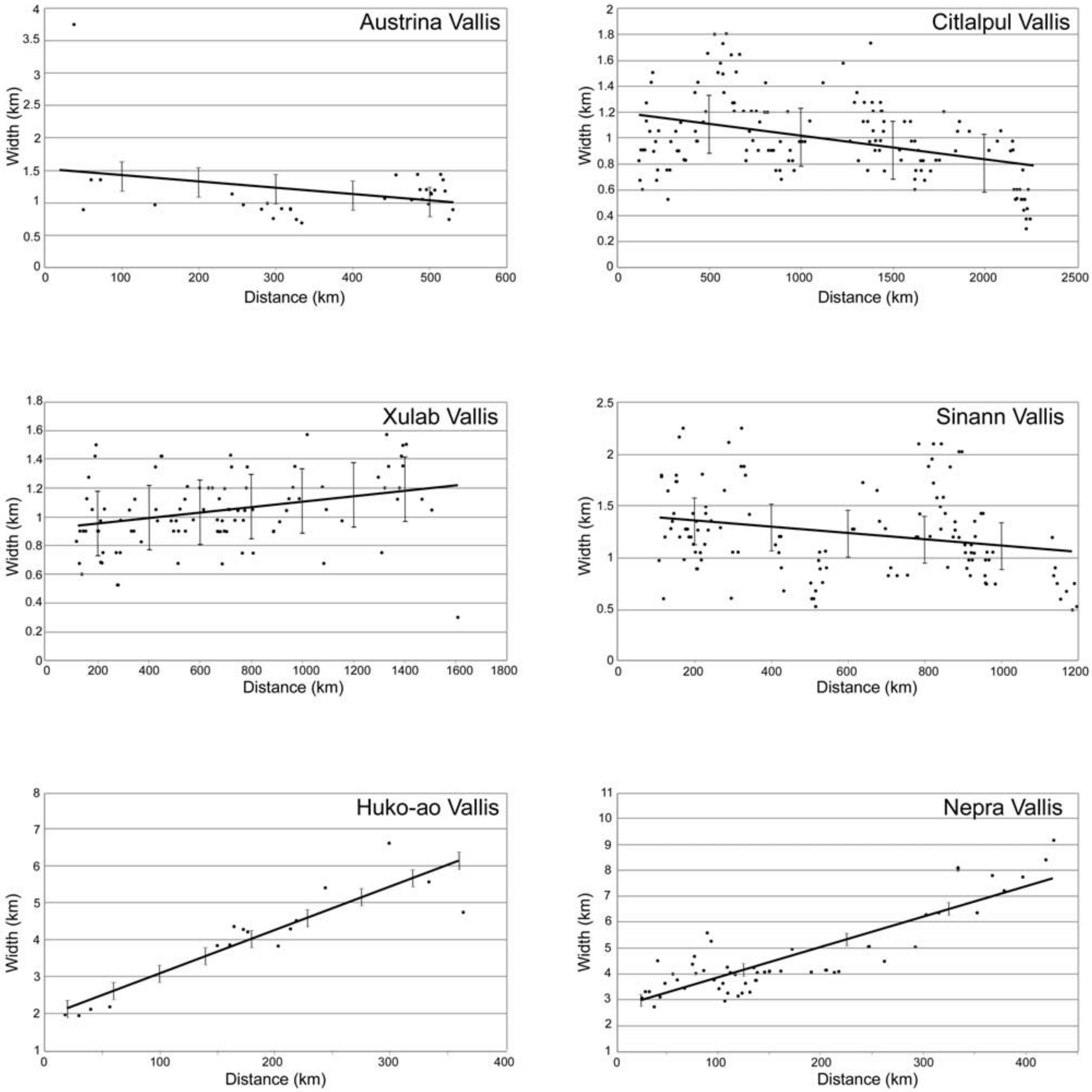


**Figure 9.** (continued)

flow is halted by topographic (or other) obstacles, the continued eruption at the vent will initiate pooling of lava down-stream. This causes an increase in width as the flow front expands to accommodate the growing volume of magma. If effusive activity continues, the buildup of pressure down-channel will cause a breach in the tube ceiling: a ''break out.'' The lava flow can then continue, perhaps with a change in direction. However, if this is the case, one might expect a corresponding variation in the radius of curvature at these points, which is not observed. It is also doubtful that the lava tubes would then collapse so completely to form such coherent channels. Although separation of channel sections has been noted by *Lang and Hansen* [2006], most canali sampled in his work appeared close to continuous, which would therefore require complete collapse of lava tubes in order to form canali.

[37] Variation of ground slope also affects channel width, causing liquids to pool in areas of low topography. Tectonism during late canali formation would cause the pooling of the canali-forming agents into regions of low topographic relief, creating wider channel sections. Most canali display localized width increases that could be the result of this type of pooling. However, further investigation of the local topography is necessary to confirm this, and such ponding would not explain the large-scale cyclic variance noted in Figure 10b.

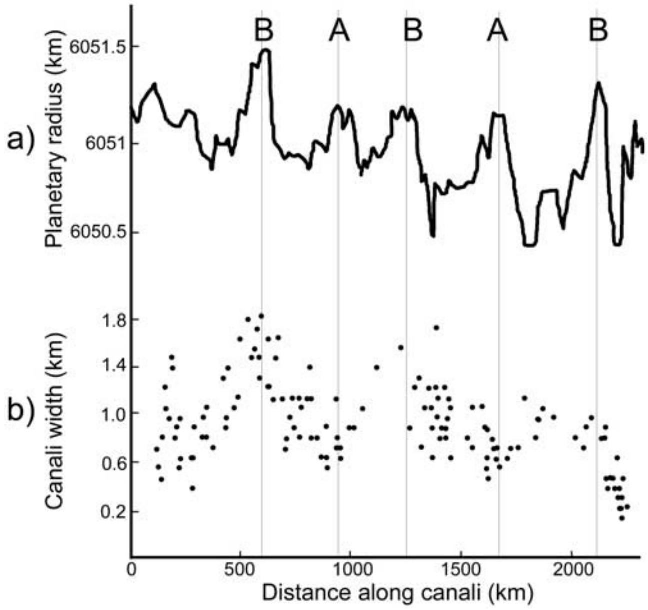


**Figure 10.** (a) Altitude data along Citlalpul Vallis from *Komatsu and Baker* [1994b]. (b) Width measurements along the length of the channel. Sheer vertical lines pick out the correlations between peaks in the average width trend and the topographic peaks marked B. Width minima correlate to the topographic peaks marked A.

[38] The topographic elevations of two canali investigated in this work were recorded by *Komatsu and Baker* [1994b]. The major peaks in topography approximately correspond to width maxima and minima. The trend is especially prominent for Citlalpul Vallis, the canali-type channel in Figure 10, in which the topographic highs coincide with width maxima and minima alternately, possibly reflecting two stages of deformation. If the canali were affected by plains tectonism then Figure 10 suggests that those topographic highs marked "A" rose first. The canali then widened in the lower areas before a second phase of tectonism raised the peaks marked "B." The fact that all maxima in the average width trend do not correlate to topographic highs reinforces that these width changes are not a result of tectonic extension occurring at the crest of topography to locally widen the channels. Citlalpul Vallis has been studied in detail by *Johnson et al.* [1999] and, with nearby Xulab Vallis, appears to have changed in both width and course during the channels formation. The fact that these changes can be connected with longitudinal profiles (for widths) or regional profiles (for courses) is another indication that the canali formation timescales in this area somehow correspond to those of plains tectonism (G. Komatsu, personal communication, 2006). Initiation of plains deformation while the canali were still flowing has also been suggested by *Stewart and Head* [2000] and is supported by this work.

[39] A link between present-day topography and canali width indicates that canali are younger, or stayed active longer, than previously imagined. If the latter is true then the formation of canali requires the stability of the canali-forming fluid (whether aqueous or volcanic) at the Venusian surface for a greatly extended period of time. This is consistent (though not exclusively) with the idea of canali formation by a lava of similar liquidus temperature to the Venusian surface temperature, as it allows for the lava to remain fluid during the early stages of plains tectonism.

## 4. Conclusions

[40] Analysis of the morphological features and meander geometry of canali conducted during this work support earlier results that the channels were likely formed by a fluid of water like viscosity. Further analysis of dominant meander wavelength suggests that canali formation was a rapid, large-scale event involving vast volumes of lava, flowing at a rate of up to $6.6 \times 10^6$ $m^3$ $s^{-1}$. Inner channels and evidence of canali being affected by plains tectonism suggests that flow activity or fluidity was sustained after this initially rapid period of channel formation.

[41] When compared to other Venusian channels, negligible change in width along canali length indicates that the rheology and volume of the canali-carving fluid remained relatively constant. This requires the canali-carving fluid to be stable at the Venusian surface for an extended period of time. In order for lava to create the extensive canali, the lava must have been sustained above its liquidus temperature for that time, allowing for constant rheological properties to be maintained and avoiding viscosity increase through cooling. Canali formation via volcanic processes under current Venusian conditions therefore relies upon the action of a lava with a liquidus value below 470°C. However, if surface temperatures were higher on Venus in the past, lavas with higher liquidus temperatures could also have formed the canali-type channels.

[42] The continued activity inferred from the presence of inner channels within canali suggests that flow volume estimates based purely on approximate canali dimensions are likely to be a lower bound. Furthermore, the canali in this work display a subtle decrease in width along their length, possibly indicating the role of downstream loss mechanisms. This implies that the total volume of fluid carried by the canali is even larger than previously realized, posing a further problem for models involving lavas.

[43] **Acknowledgments.** We thank G. Komatsu and N. P. Lang for their thoughtful and constructive reviews that significantly helped improve the quality of this manuscript. Discussions with V. R. Baker, M. Balme, and D. Waltham also proved invaluable.

## References

Baker, V. R., G. Komatsu, T. J. Parker, V. C. Gulick, J. S. Kargel, and J. S. Lewis (1992), Channels and valleys on Venus: Preliminary analysis of Magellan data, *J. Geophys. Res.*, *97*(E8), 13,421–13,444.

Baker, V. R., G. Komatsu, T. J. Parker, and V. C. Gulick (1997), Channels and valleys on Venus, in *Venus II*, edited by S. W. Bougher, D. M. Hunten, and R. J. Phillips, pp. 757–793, Univ. of Ariz. Press, Tucson.

Basilevsky, A. T., and J. W. Head (1996), Evidence for rapid and widespread emplacement of volcanic plains on Venus: Stratigraphic studies in the Baltis Vallis region, *Geophys. Res. Lett.*, *23*, 1497–1500.

Bullock, M. A., and D. H. Grinspoon (2001), The recent evolution of climate on Venus, *Icarus*, *150*, 19–37.

Bussey, D. B. J., S. A. Sorenson, and J. E. Guest (1995), Factors influencing the capability of lava to erode its substrate: Application to Venus, *J. Geophys. Res.*, *100*(E8), 16,941–16,948.

Carr, M. H. (1974), Role of lava erosion in the formation of lunar rilles and Martian channels, *Icarus*, *22*, 1–23.

Clark, J. D., and K. T. Pickering (1996), Architectural elements and growth patterns of submarine channels: Application to hydrocarbon prospectivity, *AAPG Bull.*, *80*, 194–221.

Dury, G. H. (1964), Principles of underfit streams, *U. S. Geol. Surv. Prof. Pap.*, *452-A*, 1–67.

Garry, W. B., and K. P. Gregg (2005), Analysis of downstream transitions in morphology and structure of lava channels on Mars, *Lunar Planet. Sci.*, *XXXVI*, Abstract 2019.

Genge, M., A. P. Jones, and G. D. Price (1995), An infrared and Raman study of carbonate glasses: Implications for the structure of carbonatite magmas, *Geochim. Cosmochim. Acta*, *59*, 927–937.

Gregg, T. K. P., and R. Greeley (1993), Formation of Venusian canali: Considerations of lava types and their thermal behaviors, *J. Geophys. Res.*, *98*(E6), 10,873–10,882.

Hulme, G. (1974), The interpretation of lava flow morphology, *Geophys. J. Astron. Soc.*, *39*, 361–383.

Johnson, J. R., G. Komatsu, and V. R. Baker (1999), Geologic map of the Barrymore Quadrangle (V59), Venus, *U. S. Geol. Surv. Geol. Invest. Ser.*, *I-2610*.

Jones, A. P., and K. T. Pickering (2003), Evidence for aqueous fluid-sediment transport and erosional processes on Venus, *J. Geol. Soc.*, *160*, 1–9.

Kargel, J. S., B. J. R. Fegley, A. Treiman, and R. L. Kirk (1994), Carbonate-sulfate volcanism on Venus?, *Icarus*, *112*, 219–252.

Kereszturi, A. (2003), Paleodischarge estimation from morphometry of ancient channels, in *Sixth International Conference on Mars*, Abstract 3039, Lunar and Planet. Inst., Houston, Tex.

Komatsu, G., and V. R. Baker (1994a), Meander properties of Venusian channels, *Geology*, *22*, 67–70.

Komatsu, G., and V. R. Baker (1994b), Plains tectonism on Venus: Inferences from longitudinal profiles, *Icarus*, *110*, 275–286.

Komatsu, G., and V. R. Baker (1996), Channels in the solar system, *Planet. Space Sci.*, *44*, 801–815.

Komatsu, G., J. S. Kargel, and V. R. Baker (1992), Canali-type channels on Venus: Some genetic constraints, *Geophys. Res. Lett.*, *19*, 1415–1418.

Komatsu, G., V. R. Baker, V. C. Gulick, and T. J. Parker (1993), Venusian channels and valleys: Distribution and volcanological implications, *Icarus*, *102*, 1–25.

Lang, N. P., and V. L. Hansen (2006), Venusian channel formation as a subsurface process, *J. Geophys. Res.*, *111*, E04001, doi:10.1029/2005JE002629.

Leopold, L. B., and M. G. Wolman (1957), River channel patterns: Braided, meandering and straight, *U. S. Geol. Surv. Prof. Pap.*, *282-B*, 39–85.

Leopold, L. B., and M. G. Wolman (1960), River meanders, *Geol. Soc. Am. Bull.*, *71*, 769–794.

Oshigami, S., and N. Namiki (2005), Cross-sectional profile of Baltis Vallis channel on Venus: Reconstruction from Magellan SAR brightness data, *Lunar Planet. Sci.*, *XXXVI*, Abstract 1555.

Robie, R. A., B. S. Hemingway, and J. R. Fisher (1978), Thermodynamic properties of mineral and related substances at 298.15 K and 1 bar pressure and at higher temperatures, *U. S. Geol. Surv.*, *1452*.

Rossi, M. J. (1997), Morphology of the 1984 open-channel lava flow at Krafla volcano, northern Iceland, *Geomorphology*, *20*, 95–112.

Schumm, S. A. (1977), *The Fluvial System*, John Wiley, Hoboken, N. J.

Schumm, S. A., and R. F. Hadley (1957), Arroyos and the semiarid cycle of erosion, *Am. J. Sci.*, *256*, 161–174.

Stewart, E. M., and J. W. Head (2000), Evidence for the temporal continuity of deformation in the Baltis Vallis region of Venus from observations of canali topography, *Lunar Planet. Sci.*, *XXXI*, Abstract 1692.

William-Jones, G., and J. Stix (1994), The meandering canali of Venus, *Eos Trans. AGU*, *75*(44), Fall Meet. Suppl., 416.

William-Jones, G., A. E. William-Jones, and J. Stix (1998), The nature and origin of Venusian canali, *J. Geophys. Res.*, *103*(E4), 8545–8555.

Williams, G. P. (1986), River meanders and channel size, *J. Hydrol.*, *88*, 147–164.

Williams, R. M. E., and M. C. Malin (2004), Evidence for late stage fluvial activity in Kasei Valles, Mars, *J. Geophys. Res.*, *109*, E06001, doi:10.1029/2003JE002178.

Wohl, E. E., and H. Achyuthan (2002), Substrate influence on incised channel morphology, *J. Geol.*, *110*, 115–120.

V. J. Bray and R. C. Ghail, Department of Earth Science and Engineering, Imperial College London, South Kensington, London SW7 2BP, UK. (veronica.bray@imperial.ac.uk)

D. B. J. Bussey, Applied Physics Laboratory, 11100 Johns Hopkins Road, Laurel, MD 20723, USA.

A. P. Jones and K. T. Pickering, Department of Earth Sciences, University College London, Gower Street, London WC1E 6BT, UK.